Kinetic Analysis by Fluorescence of the Interaction between Ras and the Catalytic Domain of the Guanine Nucleotide Exchange Factor $Cdc25^{Mm}$ †

Christian Lenzen,‡ Robbert H. Cool,*,‡ Heino Prinz, Jürgen Kuhlmann, and Alfred Wittinghofer

Max-Planck-Institut für molekulare Physiologie, Postfach 10 26 44, 44126 Dortmund, Germany

Received October 22, 1997; Revised Manuscript Received February 3, 1998

ABSTRACT: Guanine nucleotide exchange factors (GEFs) activate Ras proteins by stimulating the exchange of GTP for GDP in a multistep mechanism which involves binary and ternary complexes between Ras, guanine nucleotide, and GEF. We present fluorescence measurements to define the kinetic constants that characterize the interactions between Ras, GEF, and nucleotides, similar to the characterization of the action of RCC1 on Ran [Klebe et al. (1995) *Biochemistry 34*, 12543−12552]. The dissociation constant for the binary complex between nucleotide-free Ras and the catalytic domain of mouse Cdc25, $Cdc25^{Mm285}$, was 4.6 nM, i.e., a 500-fold lower affinity than the Ras·GDP interaction. The affinities defining the ternary complex Ras·nucleotide·$Cdc25^{Mm285}$ are several orders of magnitude lower. The maximum acceleration by $Cdc25^{Mm285}$ of the GDP dissociation from Ras was more than 10^5-fold. Kinetic measurements of the association of nucleotide to nucleotide-free Ras and to the binary complex Ras·$Cdc25^{Mm285}$ show that these reactions are practically identical: a fast binding step is followed by a reaction of the first order which becomes rate limiting at high nucleotide concentrations. The second reaction is thought to be a conformational change from a low- to a high-affinity nucleotide binding conformation in Ras. Taking into consideration all experimental data, the reverse isomerization reaction from a high- to a low-affinity binding conformation in the ternary complex Ras·GDP·$Cdc25^{Mm285}$ is postulated to be the rate-limiting step of the GEF-catalyzed exchange. Furthermore, we demonstrate that the disruption of the Mg^{2+}-binding site is not the only factor in the mechanism of GEF-catalyzed nucleotide exchange on Ras.

One of the essential processes in signal transduction pathways via Ras or Ras-like proteins is their activation by guanine nucleotide exchange factors (GEFs).[1] These proteins act as stimulators of the slow intrinsic dissociation rate of the Ras·nucleotide complexes. Since the cellular concentration of GTP is higher than that of GDP and the affinity of Ras for GTP is slightly higher than that for GDP, GTP will bind to Ras, thereby activating the Ras protein. Only the Ras·GTP complex can bind with high affinity to its downstream effectors and thus transmit a signal. Several genes have been isolated from different organisms encoding proteins that have a GEF activity specific for Ras (for which we use the general name RasGEFs throughout this paper): SOS1 and SOS2 (*1*−*4*); $Cdc25^{Mm}$, also called RasGrf (*5*−*7*); and mRas-GRF2 (*8*). Another cloned putative RasGEF, C3G (*9*), turned out to be a Rap1-specific GEF (*10*, *11*). The RasGEFs are proteins of considerable length, 120−160 kDa, and contain several regions which are generally accepted to represent structural domains (*12*). A region of 200−300 amino acids, the RasGEF domain, is shared by all GEFs which act on members of the Ras subfamily, and their activity is specific toward either Ras, Ral, or Rap. The fact that truncated versions of various lengths, containing this RasGEF domain, have been shown to be active RasGEFs in vivo and in vitro (*4*, *13*−*16*) confirms that this region indeed represents the Ras-specific guanine nucleotide exchange domain.

It has been proposed that RasGEFs stimulate the slow intrinsic dissociation rate of the Ras·nucleotide complex via the formation of a ternary Ras·nucleotide·GEF and a binary Ras·GEF complex. GTP then binds to the binary complex, which in turn releases the GEF from the resulting ternary complex (Scheme 1; see Results) (*17*), as proposed for the action of $CDC25^{Sc}$ and $SDC25^{Sc}$, the exchange factors of the Ras homologue RAS2 in yeast *Saccharomyces cerevisiae* (*18*), of EF-Ts, the exchange factor of the *Escherichia coli* elongation factor Tu (*19*), and of RCC1, the Ran-specific GEF (*20*). Somewhere along the reaction pathway the tightly bound nucleotide (with a K_D in the picomolar range for Ras and Ran) must become loosely bound for the fast dissociation to occur. For the RCC1-catalyzed nucleotide exchange reaction on Ran, one or more conformational transitions from

† R.H.C. was supported by EC Grants EC Bio2-CT93-0005 and Bio4-CT96−1110.

* Corresponding author. Telephone: (49)231-1206524. Fax: (49)-231-1206230. E-mail: robbert.cool@mpi-dortmund.mpg.de.

‡ These authors contributed equally.

[1] Abbreviations: $Cdc25^{Mm285}$, catalytic domain of the mouse guanine nucleotide exchange factor $Cdc25^{Mm}$ comprising the C-terminal 285 amino acids, preceded by the peptide Gly-Ser; DTE, dithioerythiol; GEF, guanine nucleotide exchange factor; RasGEF, Ras-specific GEF; mGDP, mGTP, or mGppNHp, GDP, GTP, or homologue GppNHp, respectively, carrying the mant group on the 2′- or 3′-hydroxyl group of the ribose; 3′mdGDP or 3′mdGTP, dGDP or dGTP with the mant group attached to the 3′-OH group; GST, glutathione-*S*-transferase; mant, *N*-methylanthraniloyl; Ras, recombinant protein encoded by the H-Ras gene, isolated from *Escherichia coli*.

S0006-2960(97)02621-4 CCC: $15.00
Published on Web 04/28/1998

a tightly to a loosely bound nucleotide state with a concomitant change from a loosely to a tightly bound GEF have been proposed (*20*).

Although the stimulatory effect of GEFs on the intrinsic dissociation rate of Ras proteins has been documented rather extensively, a full kinetic analysis of the reaction in solution rather than on nitrocellulose membranes is lacking as yet. We have developed kinetic and equilibrium methods to study the interaction of Ran·nucleotide complexes with the Ran-specific GEF RCC1 (*20*), using fluorescence measurements with guanine nucleotides carrying the fluorescent mant group on the ribose. We have shown before that the GEF-catalyzed nucleotide exchange reaction on Ras is not perturbed by the fluorescent reporter group (*21*). Here we present the results with a similar system for the characterization of the action of the catalytic portion of the mouse GEF, Cdc25^{Mm}, on recombinant H-Ras.

MATERIALS AND METHODS

Production and Isolation of Proteins. Cdc25^{Mm285} was expressed as a GST fusion protein from pGEX2T-CDC25-12 in the protease-negative *E. coli* strain AD202 (ompT:: Tn5; 22); plasmid and cells were kindly provided by Dr. E. Martegani and Dr. T. Saito, respectively. The GEF was isolated and purified in the nonfused form as described (*21*), but in the presence of 10% glycerol (*16*). At the end, Cdc25^{Mm285} was concentrated, dialyzed against standard buffer (40 mM Na-HEPES, pH 7.6, 10 mM $MgCl_2$, and 5 mM DTE), centrifuged to remove insoluble protein, shock-frozen in liquid nitrogen, and kept at −80 °C.

The protein H-Ras was produced from the plasmid ptacras in CK600K as described (*21*). The GST−Ras fusion protein used in the BiaCore experiments was produced from the plasmid pGEX2T-Ras, a generous gift from Dr. A. Parmeggiani. The expression of GST−Ras in AD202 and purification using a GSH−Sepharose column and a gel filtration column were performed by the standard protocol for GST fusion proteins. The protease inhibitor Pefablock (Merck, Darmstadt, Germany) was added to the chromatography buffers, as well as 5 mM $MgCl_2$ for stabilization of the Ras· nucleotide complex. Purified recombinant K- and N-Ras were kindly donated by Dorothee Vogt.

The binary complex Ras·Cdc25^{Mm285} was made by incubating Ras·GDP in a slight molar excess to Cdc25^{Mm285} in standard buffer containing 10 mM EDTA for 30 min at room temperature. Thereafter, the sample was loaded onto a Superdex 75 column (Pharmacia); equilibrated with 50 mM Tris-HCl, pH 7.5, 150 mM NaCl, 1 mM EDTA, and 5 mM DTE; and eluted with the same buffer to separate the complex from the free components. Finally, the complex was concentrated; dialyzed against 50 mM Tris-HCl, pH 7.5, and 5 mM DTE; aliquoted; shock-frozen; and kept at −80 °C.

Nucleotide Exchange on Ras Proteins. The synthesis of mant-nucleotides and the exchange reaction on Ras proteins was done as described (*21*).

Kinetic Measurements Using Fluorescence. All kinetic measurements were carried out in standard buffer and at 20 °C, unless otherwise indicated.

(A) Dissociation Rates. The intrinsic and Cdc25^{Mm285}-stimulated dissociation rates were measured as described (*21*). The data were fitted with the program GraFit (Eritacus) to the single-exponential function $F_t = A_0e^{-kt}$ + offset [with offset as the fluorescence value at infinite time, A_0 as the amplitude (= $F_{t=0}$ − offset), t as the time, and k as the apparent dissociation rate constant]. Initial rates (V_0; see Figure 2) were determined by linear analysis of the fluorescence data obtained directly after mixing (first 10−40 s).

(B) Association Rates. Association rates were measured at 20 °C in the two-channel modus on the SF61 stopped-flow apparatus (Hi-Tech). The first channel measured the transmission at 365 nm, to evaluate possible aggregation of protein in time. The second channel was used to measure the fluorescence (excitation wavelength, 365 nm; emission measured with cutoff filter WK399). The system was calibrated with a mant-nucleotide solution of known concentration. After the calibration, the first syringe was filled with standard buffer containing a 4 μM solution of Ras-nf or Ras·Cdc25^{Mm285}, and the second syringe, with solutions of different nucleotide concentrations: 1, 4, 16, 32, and 64 μM. The reaction was started by mixing the solutions from the two syringes in a 1:1 ratio in the stopped-flow apparatus within 2 ms. For every nucleotide concentration 6−8 measurements of 25 s were recorded in a logarithmic time scale. Both the transmission and the fluorescence data were averaged. To correct for the inner filter effect observed at higher nucleotide concentrations, the transmission values obtained with the lowest concentration of nucleotide (0.5 μM after mixing) were taken as reference ($T_{100\%}$) and the following equation was applied:

$$F_{corr} = F_{exp}T_{100\%} \times 2/(T_{100\%} + T_x[C])$$

F_{exp} denotes the observed fluorescence signal, and $T_x[C]$ the observed transmission at the particular nucleotide concentration. The corrected fluorescence data (shown in Figure 6) were used for curve fitting on the basis of the required set of differential equations (see below). They were also used for an independent exponential analysis with the observed rate constants k_{obs} plotted as a function of nucleotide concentration and fitted to a hyperbolic function as described earlier (*23*).

Equilibrium Titrations Using Fluorescence. Titrations of the Ras·3′mdGDP with Cdc25^{Mm285} were carried out with a Fluoromax SPEX fluorometer by adding increasing amounts of GEF to 2 mL of 10 nM Ras·3′mdGDP in standard buffer. The solution was carefully mixed and the fluorescence signal (excitation wavelength, 366 nm; emission wavelength, 442 nm) was measured for typically 5−10 min to ascertain that a stable value was obtained. At the end of the titration the end point was determined by adding a 500-fold excess of GDP. The total volume of added Cdc25^{Mm285} and GDP was less than 50 μL.

The data obtained were fitted with the multiparameter-fitting program FACSIMILE (AEA Technology, Harwell, Didcot, Oxfordshire OX11 ORA, U.K.). Under equilibrium conditions, different conformational states of a given complex are in equilibrium with each other, so that reaction Schemes 1 and 4 (or even more complicated schemes) cannot be distinguished. Therefore, the simplest reaction scheme as depicted in Scheme 1 was applied. Here, the dissociation constants are defined as: K_D1 = [R][G]/[RG]; K_D2 = [R][C]/[RC]; K_D3 = [RG][C]/[RCG]; and K_D4 = [RC][G]/[RCG], with the letters symbolizing the concentra-

Scheme 1

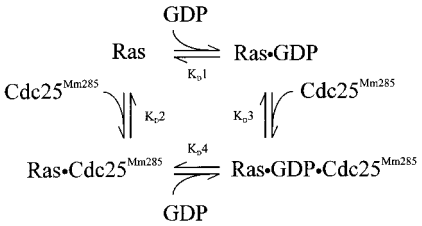

tions of Ras [R], guanine nucleotide [G], and $Cdc25^{Mm285}$ [C], or their complexes. The four dissociation constants are related by the equation $K_D1/K_D2 = K_D4/K_D3$ (*20*).

The fluorescent mant-nucleotides (M) were initially assumed to possess affinities differing from the nonfluorescent nucleotides (G). However, our data did not justify these additional parameters, so that K_D1 = [R][G]/[RG] and K_D4 = [RC][G]/[RCG] were used for both fluorescent and nonfluorescent nucleotides. Numerically, it was more convenient to use the corresponding differential equations with the program FACSIMILE and to calculate for 1000 s with the assumption of fast association rate constants (in all cases: 10^7 M^{-1} s^{-1}). Furthermore, a quotient representing the relative quantum yield of the fluorescence signal of the mant-nucleotide bound to Ras and to Ras•$Cdc25^{Mm285}$ was introduced. All programs are available as FACSIMILE files upon request.

BiaCore Measurements. The surface of a sensor chip, CMS research grade (Pharmacia), was activated and charged with anti-GST serum (Pharmacia) as described (*24*). In standard buffer, the binding capacity was not very stable: after each regeneration, but also in time during one measurement, a significant decrease in binding was observed apparently due to loss of coupled anti-GST antibody. However, when buffer containing 20 mM Na-HEPES, pH 7.4, 150 mM NaCl, 5 mM $MgCl_2$, and 0.005% Surfactant P20 was used, a much smaller loss in binding capacity in time was observed.

The proteins were diluted in buffer to the appropriate concentration and kept at 4 °C. The chip lane was charged with nucleotide-free GST−Ras by first passing 35 μL of 1 μM GST−Ras•GDP, and subsequently passing 40 mM EDTA in buffer for 6 min. The flow rate was 5 μL/min. Control experiments by fluorescence showed that, under these conditions, Ras was 95% nucleotide-free. Hereafter, an injection of $Cdc25^{Mm285}$ was performed and the binding of $Cdc25^{Mm285}$ to GST−Ras was measured as a change in resonance signal in time. Subsequently, the dissociation of the complex was studied by passing buffer over the lane. This way, the binding and dissociation kinetics of $Cdc25^{Mm285}$ to and from GST−Ras was measured. At the end of the measurement, the chip lane was recycled by passing 20 mM glycine, pH 2.0, and subsequently 0.05% SDS (4 min each), followed by a new charging with nucleotide-free GST−Ras and a new binding experiment. This way, the effect of several concentrations of $Cdc25^{Mm285}$ on the surface plasmon resonance were measured.

The association and dissociation rate constants were calculated using the program BIAlogue 1.4 (Pharmacia).

RESULTS

Protein Purification. $Cdc25^{Mm285}$ was purified basically as described (*21*) in the presence of 10% glycerol (*16*), concentrated to 5−15 mg/mL, dialyzed against standard buffer, shock-frozen in liquid nitrogen in aliquots, and kept at −80 °C. It was important to keep the highly concentrated protein on ice. At room temperature an aggregation occurred, giving the protein solution a milky appearance, which disappeared as soon as the solution was recooled on ice and/or diluted. This reversible aggregation is probably caused by hydrophobic interactions, which are favored at higher temperatures. No significant alteration of the GEF activity of $Cdc25^{Mm285}$ could be measured after reversion of the aggregation.

Table 1: Specificity of Interaction between $Cdc25^{Mm285}$ and the Three Ras Isoforms H-, K-, and N-Ras[a]

	intrinsic dissociation rate (10^{-5} s^{-1})	dissociation rate in the presence of 50 nM $Cdc25^{Mm285}$ (10^{-5} s^{-1})	fold stimulation
H-Ras•mGDP	1.2	56	47
K-Ras•mGDP	1.6	62	39
N-ras•mGDP	1.0[b]	84	84

[a] Catalysis of nucleotide dissociation by $Cdc25^{Mm285}$ was measured at 20 °C with 100 nM Ras•mGDP, 20 μM GDP, and 50 nM GEF in 50 mM Tris-HCl, pH 7.6, 5 mM $MgCl_2$, and 5 mM DTE. [b] The fluorescence signal of N-ras•mGDP in the presence of excess GDP decreases with a rate of 1.4×10^{-5} s^{-1} and in the absence of excess GDP with a rate of approximately 0.4×10^{-5} s^{-1}. Thus, the corrected intrinsic dissociation rate is 1.0×10^{-5} s^{-1}.

Temperature Stability of $Cdc25^{Mm285}$. To determine the temperature stability of $Cdc25^{Mm285}$, we have measured the $Cdc25^{Mm285}$-stimulated dissociation of 1 μM Ras•mGDP in standard buffer containing 1 μM $Cdc25^{Mm285}$ and 200 μM GDP at temperatures ranging from 5 to 42 °C. As expected, the GEF activity of $Cdc25^{Mm285}$ increased with increasing temperatures up to 30 °C, but at higher temperatures a rapid decrease of activity was observed (not shown). We have performed all further experiments at 20 °C to avoid this decay.

Specificity. Three mammalian isoforms of Ras, H-, K-, and N-Ras, have been identified which are highly conserved in their primary sequence. The significance of having more than one isoform is not understood at present, although the isoforms may have different functions in different tissues, since certain types of tumors have a preference for a particular activated Ras gene, such as K-Ras for lung, colon and pancreas cancers and N-Ras for myeloid leukemias (*25*). To see whether $Cdc25^{Mm285}$ acts differently on the three isoforms, we tested the GEF activity of $Cdc25^{Mm285}$ on these proteins. As summarized in Table 1, $Cdc25^{Mm285}$ is active on all isoforms, being somewhat more active on N-Ras, in accordance with the results of Leonardsen et al. (*26*).

Dependence of the Exchange Reaction on the Nature of Bound and Unbound Nucleotide. It has been reported that GEFs specifically facilitate the formation of the GTP-bound state, by being more active on the GDP-bound than the GTP-bound form of Ras (*13*, *27*). However, for the Ran/RCC1 system we could show that RCC1 merely functions as a catalyst that decreases the time needed for reaching equilibrium between the GDP- and GTP-bound states (*20*). Therefore, we tested the nucleotide specificity of the interaction of $Cdc25^{Mm285}$ with Ras. Figure 1 shows the release of Ras-bound 3′mdGDP or 3′mdGTP (4 μM), in the presence of an excess of unlabeled nucleotide and in the presence or

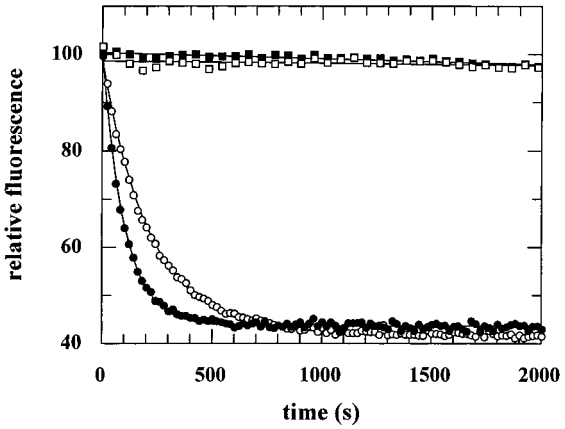

FIGURE 1: Effect of the bound nucleotide on the stimulated exchange reaction. Ras·3′mdGDP (4 μM) (closed symbols) or Ras·3′mdGTP (4 μM) (open symbols) was incubated in standard buffer containing 10 μM GDP or GTP at 20 °C in the presence (circles) or absence (squares) of 1 μM Cdc25^{Mm285}. The decrease of fluorescence emission at 450 nm due to dissociation of fluorescent nucleotide was followed with time, and the rates were fitted to single exponentials.

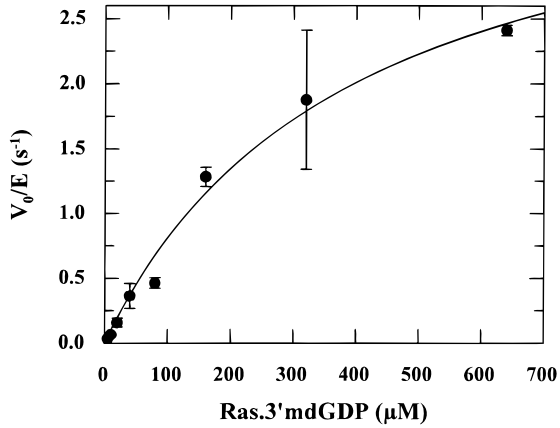

FIGURE 2: Saturation of the Cdc25^{Mm285}-catalyzed dissociation of Ras·3′mdGDP. A constant concentration of Cdc25^{Mm285} (1 μM) was incubated with increasing concentrations of Ras·3′mdGDP, as indicated, and a 100-fold excess of GDP. Initial dissociation rates (V_0) were measured at least twice at each concentration of Ras as described in Materials and Methods, and the mean values were plotted against the Ras·3′mdGDP concentration. *E* stands for the concentration of Cdc25^{Mm285} (1 μM). The data were fitted to a hyperbolic equation.

absence of 1 μM Cdc25^{Mm285}. The Cdc25^{Mm285}-stimulated dissociation rate of Ras·3′mdGDP is approximately twice that of Ras·3′mdGTP, with values of 0.0098 and 0.0046 s^{-1}, respectively. However, since the intrinsic dissociation rate of Ras for GTP (1×10^{-5} s^{-1}) is 2-fold lower than that for GDP (2×10^{-5} s^{-1}), the stimulatory action of Cdc25^{Mm285} is practically independent of the nature of the bound nucleotide. The difference in stimulated dissociation rates is somewhat smaller than the results of Jacquet et al. (*16*) but is similar to the results with the yeast proteins CDC25 and RAS2 obtained by Haney and Broach (*28*).

To measure the limiting rate of the exchange reaction under multiple-turnover conditions, increasing concentrations of up to 600 μM Ras·GDP (the substrate) were used in the presence of 1 μM exchange factor (the enzyme). The initial rates were plotted as a function of the Ras·nucleotide concentration (Figure 2), and the data were fitted with a hyperbolic function [$A = A_0L/(L + K_m)$, with A as the initial rate at the specific Ras concentration, A_0 as the maximum rate, L as the Ras concentration, and K_m as the apparent Michaelis−Menten constant]. Although we did not reach complete saturation at 600 μM Ras·nucleotide, the data could be fitted to obtain a maximal rate of 3′mdGDP release from Ras of 3.9 s^{-1} and an apparent K_m value of 386 μM. Since the intrinsic dissociation rate of 3′mdGDP is 2×10^{-5} s^{-1} (Table 1), the acceleration of GDP dissociation from Ras by this GEF is approximately 2×10^5-fold. An apparent K_m of approximately 300 μM was obtained for the triphosphate-bound form of Ras, confirming that there is no pronounced specificity toward the nature of the Ras-bound nucleotide (data not shown).

It has been suggested that the rate of guanine nucleotide release from Ras is dependent on free nucleotide (*28*), which is somewhat surprising considering the fact that nucleotide dissociation rates are usually much lower than nucleotide association rates, even for very weakly binding mutants of Ras such as F28L and S17A (*29, 30*). We therefore tested whether the release of fluorescent nucleotide is influenced by the concentration and nature of unbound nucleotide. Varying the excess of nucleotide between 10 and 10 000-fold did not affect the observed Cdc25^{Mm285}-stimulated dissociation rate, nor could we observe a difference in effect when excess GDP or GTP was used for the exchange reaction (not shown). In these experiments, the buffer contained 20 mM $MgCl_2$ to saturate the nucleotide with Mg^{2+} even at the highest concentration of nucleotide (10 mM).

Equilibrium Titration of Ras·3′mdGDP with Cdc25^{Mm285}. The mechanism for interaction of Ras with guanine nucleotide and Cdc25^{Mm285} can be described in the simplest way by Scheme 1, in analogy to the interaction of Ran, RCC1, and guanine nucleotide (*20*). Since we are measuring under equilibrium conditions, Scheme 1 also covers more complicated reaction schemes, e.g., Scheme 4 (below). In the equilibrium titration, we added increasing amounts of Cdc25^{Mm285} to a given concentration of fluorescently labeled Ras·3′mdGDP. We have used 3′mdGDP in these experiments because (ribo)mGDP, which is a mixture of 2'- and 3'-mant-GDP isomers, can produce unwanted side effects (*31*). As can be seen in Figure 3, the added GEF competes with nucleotide for binding to Ras, causing a decrease in fluorescence. At the end of the titration, an 200-fold excess of GDP was added, to determine the fluorescence due to unbound mant-nucleotide. The fluorescence above this signal stems from mant-nucleotide bound to Ras and/or the binary complex Ras·Cdc25^{Mm285}.

We have fitted our data to reaction Scheme 1, as described in Materials and Methods. The equilibrium dissociation constant for Ras·3′mdGDP (K_D1) had been determined independently as 9 pM from nucleotide association and dissociation experiments (Tables 2 and 3). Experimental data used in the multiparameter program were the fluorescence data (including the fluorescence of buffer and the fluorescence after addition of excess GDP), the Cdc25^{Mm285} concentrations (as determined by Bradford, ref *31a*), and the fraction of Ras charged with 3′mdGDP (as determined by HPLC-analysis; >0.9). The introduction of differing affinities describing the ternary complex of Ras·Cdc25^{Mm285} with fluorescent and nonfluorescent nucleotides did not improve the quality of the fit. Moreover, since it is known that the

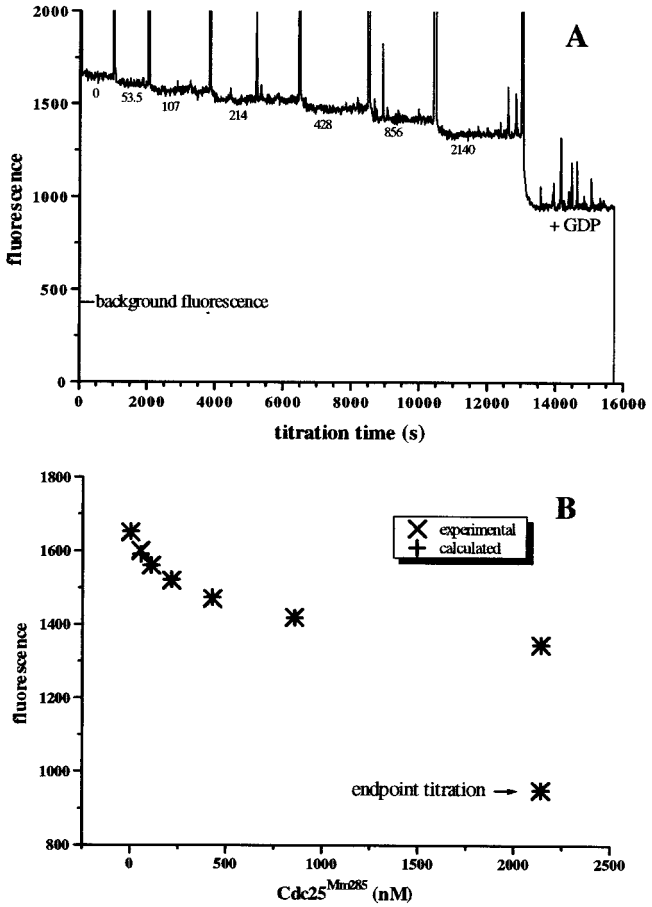

FIGURE 3: Titration of Ras·3′mdGDP with Cdc25^{Mm285} (A) Ras·3′mdGDP (10 nM) in standard buffer at 20 °C was incubated with the indicated concentrations (nM) of Cdc25^{Mm285}, and the decrease in fluorescence emmission was recorded. In the last titration step, excess GDP was added to a final concentration of 5.75 μM. (B) Correspondence of the experimental (×) values from panel A with those calculated (+) using a multiparameter fit as described in the Materials and Methods and Results.

Table 2: Equilibrium and Rate Constants Derived from the Kinetic Measurements of the Association of Nucleotide to Either Nucleotide-Free Ras (Ras-nf) or the Dimeric Complex Ras·Cdc25^{Mm285}

	Ras-nf			Ras·Cdc25^{Mm285}		
	K_D1a (μM)	k_{+1b} (s^{-1})	k_{+1} (10^6 M^{-1} s^{-1})	K_D4a (μM)	k_{+4b} (s^{-1})	k_{+4} (10^6 M^{-1} s^{-1})
3′mdGDP	11.8	26.8	2.3	8.6	20.4	2.4
3′mdGTP	10.8	23.6	2.2	8.4	20.1	2.4

presence of the fluorescent group has only a small effect on the interaction of the nucleotide with Ras (*21*, *32*) and since Ras was almost homogeneously charged with the mant-nucleotide, we have assumed that the affinities describing the ternary complex are identical for fluorescent and non-fluorescent nucleotides.

The parameters that were fitted were K_D2, K_D3, and the relative quantum yields of the fluorescent nucleotide bound to Ras and to Ras·Cdc25^{Mm285}. The best fit of our data resulted in similar quantum yields and a value of 4.6 nM for K_D2. A variation in the value for K_D2 of approximately 2-fold resulted in fits of comparable quality. In contrast to the Ran/RCC1 system, no significant amount of the ternary complex was formed over the investigated concentration

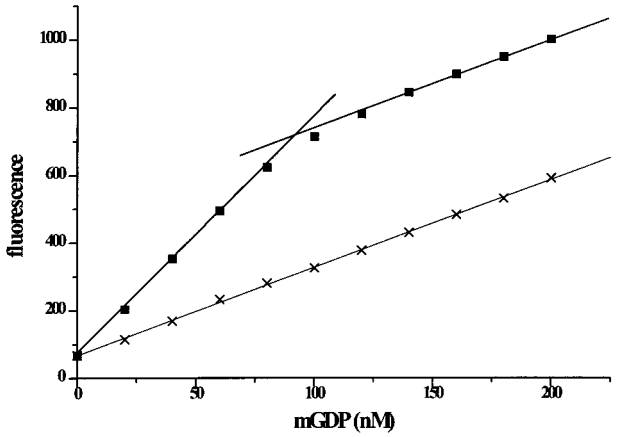

FIGURE 4: Titration of the Ras·Cdc25^{Mm285} complex with mGDP. The binary protein complex (100 nM) in 50 mM Tris-HCl, pH 7.5, 5 mM $MgCl_2$, and 5 mM DTE at 20 °C was incubated with the indicated concentrations of mGDP (■), and the increase in fluorescence emission was recorded. As a calibration, nucleotide was added to buffer alone (×).

range, so that no reliable value for K_D3 could be determined. Any K_D3 value larger than 1 μM resulted in an equally good fit.

Equilibrium Titration of Nucleotide-Free Complex Ras·Cdc25^{Mm285} with mGDP. In Figure 4 the titration of the binary complex Ras·Cdc25^{Mm285} with mGDP is shown. The increase in fluorescence emission, plotted against the concentration of added nucleotide, can be interpreted to be a resultant of two effects: the formation of Ras·nucleotide complex (steep line in Figure 4), followed by the lower increase in fluorescence due to the addition of unbound nucleotide (line parallel to the calibration curve). The sharp transition between the two lines indicates that addition of mGDP results in a direct and full binding of the nucleotide until all protein molecules have a nucleotide bound. Consequently, Ras must have a higher affinity for nucleotide than for Cdc25^{Mm285}, in accordance with the data obtained with the reverse titration as described above. Fitting of these data with the multiparameter fitting program to obtain a value for K_D2 was of no significance, since the concentrations were too high relative to K_D1 (9 pM). Unfortunately, we could not perform our experiments at concentrations in the picomolar range because the fluorescence signal would become too small. However, this type of titration can be used as an active site titration, giving the percentage of Ras in the complex that is still capable to bind nucleotide. For our complex, a value of approximately 90 nM was found at the intersection of the two lines, indicating that 90% of Ras in the complex is active in binding guanine nucleotide.

Plasmon Surface Resonance Measurements on the Ras and Cdc25^{Mm285} Interaction. Since others have reported that K_D1 and K_D2 are of similar magnitude (*16*) but the fluorescence data indicated that these constants were instead very different, we wanted to use plasmon surface resonance to obtain an independent measurement of the affinity between Ras and Cdc25^{Mm285}. We therefore coupled GST−Ras indirectly via anti-GST antibodies to the sensor chip, after which the nucleotide was released from Ras in the presence of a high excess of EDTA. The binding and release of Cdc25^{Mm285} to and from this chip was followed as shown in Figure 5. The k_{obs} values as measured from the binding of Cdc25^{Mm285}

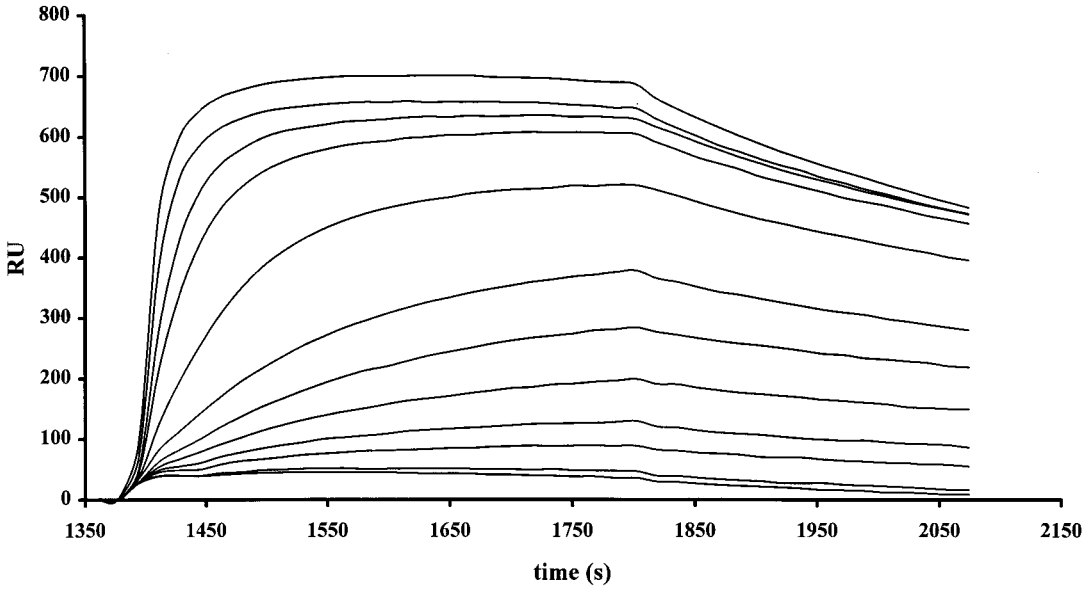

FIGURE 5: Binding of Cdc25^{Mm285} to GST−Ras-nf as measured with the BiaCore system. The biosensor chip was charged with nucleotide-free GST−Ras as described in Material and Methods, after which the association and dissociation reactions with 2, 3, 5, 7, 10, 15, 20, 40, 70, 100, 150, and 200 nM Cdc25^{Mm285} (curves from bottom to top) were measured.

Scheme 2

$$\text{Ras} + \text{GXP} \rightleftharpoons \text{Ras}\bullet\text{GXP}_\text{L} \rightleftharpoons \textit{Ras}\bullet\text{GXP}_\text{T}$$

to GST−Ras, plotted as a function of the Cdc25^{Mm285} concentration, demonstrated a linear correlation up to the highest concentration of Cdc25^{Mm285} used (500 nM, not shown). The calculated association rate constant k_{+2} was 3.3×10^5 M^{-1} s^{-1}. The dissociation rate constants were determined for each experiment, giving a mean value of 1.0×10^{-3} s^{-1} (k_{-2}). The dissociation constant K_D2 was calculated from these two values to be 3.3 nM, close to the value obtained by the fluorescence titration.

Similar experiments were carried out in standard buffer, in which the "bleeding" effect was stronger. In this case, the obtained value for K_D2 was 6.4 nM. As a control, the same experiments were carried out while charging the chip lane with GST instead of GST−Ras. No binding of Cdc25^{Mm285} was observed.

Association of Nucleotides with the Binary Ras·Cdc25^{Mm285} Complex. It has been shown before that guanine nucleotide binding to Ras involves (at least) two steps, with a fast initial binding reaction where nucleotide is bound loosely and a slow isomerization reaction to a tight-binding conformation (Scheme 2). In our reaction schemes, we have indicated the loosely and tightly bound complexes by Ras·GXP$_L$ and *Ras*·GXP$_T$, respectively. The change of fluorescence signal occurs during the second step (*23*, *33*, *34*).

The association of the fluorescent nucleotide to nucleotide-free Ras was followed by means of a stopped-flow spectrofluorometer (shown for 3′mdGTP in Figure 6A). Note the logarithmic time scale used to display all experiments and to focus on the initial part of the reaction. At low concentrations, the apparent rate constant of this reaction (inflection point in the logarithmic representation) was linearly increased with the concentrations of 3′mdGDP, as expected for a second-order association. At high concentrations of ligand, the velocity of this reaction could not be further increased, which means that the observed fluorescence increase results from a reaction of the first order, i.e., the isomerization reaction from Ras·3′mdGTP$_L$ (nucleotide bound loosely) to *Ras*·3′mdGTP$_T$ (nucleotide bound tightly)

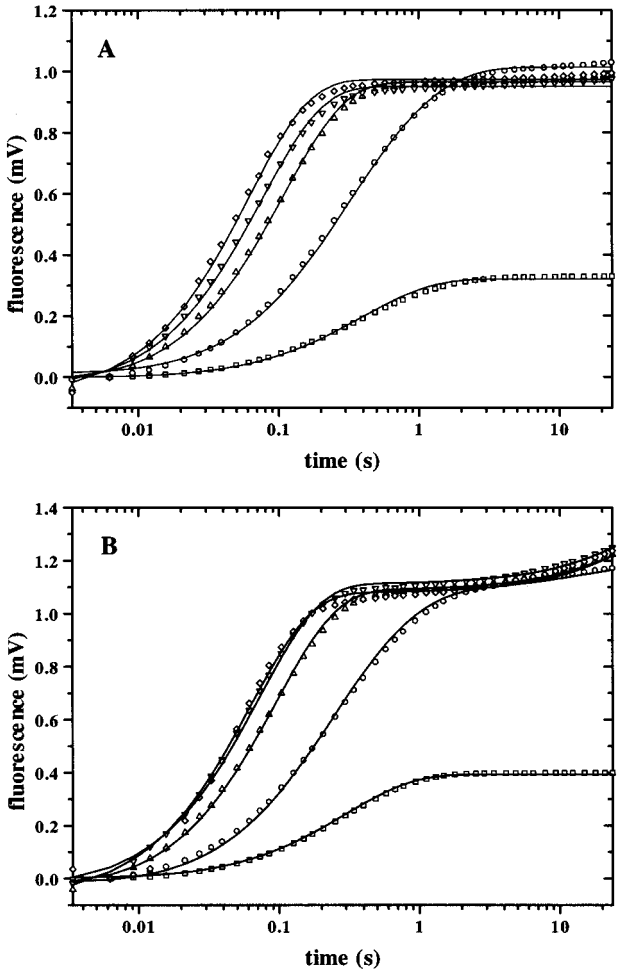

FIGURE 6: Association kinetics of nucleotide to the complex Ras·Cdc25^{Mm285} and to Ras-nf. (A) Association reaction between 2 μM nucleotide-free Ras and 0.5 (□), 2 (○), 4 (△), 8 (▽) and 16 (◇) μM 3′mdGTP in standard buffer at 20 °C. (B) Association reaction between 2 μM Ras·Cdc25^{Mm285} and increasing concentrations of 3′mdGTP (as in panel A) in standard buffer at 20 °C.

Table 3: Equilibrium and Rate Constants Derived from Fluorescence and BiaCore Experiments and from Global Fitting Procedures which Define the Interactions between Ras, Cdc25^{Mm285}, and Nucleotide

	3′mdGDP		3′mdGTP	
	data derived from individual experiments	data derived from global fit (facsimile)	data derived from individual experiments	data derived from global fit (facsimile)
K_D1 (pM)	9[a]	7.5	5[a]	3.5
K_D1a (μM)	11.8[a]	7.1	10.8[a]	7.4
K_D1b (10^{-7})	7.5[a]	10.6	4.2[a]	4.7
k_{+1b} (s^{-1})	26.8[a]	23.5	23.6[a]	21.3
k_{-1b} (10^{-6} s^{-1})	20[a]	25	10[a]	
K_D2 (nM)	3.3[b]	4.6[c]	3.3[b]	4.6[c]
k_{+2} (10^6 M^{-1} s^{-1})	0.33 [b]		0.33[b]	
k_{-2} (10^{-3} s^{-1})	1.0[b]		1.0[b]	
K_D3 (mM)	0.6	≥0.001 [c]		0.2
		0.4[d]		
K_D4 (μM)	1.6[a]	≥0.002[c]		0.3
		0.6[d]		
K_D4a (μM)	8.6[a]	3.1	8.4[a]	5.7
K_D4b (10^{-2})	19.1[a]	18.9[d]		4.6
k_{+4b} (s^{-1})	20.4[a]	20.6	20.1[a]	24
k_{-4b} (s^{-1})	3.9[e]			1.1

[a] Data obtained from association and/or dissociation reactions or calculated from such a data set. [b] Data obtained by plasmon surface resonance analysis (Biacore). [c] Data obtained from the titration experiment as described in Materials and Methods using facsimile analysis. [d] Calculated by combining data derived from individual experiments and global fit. [e] Derived as apparant k_{cat} (see text).

Scheme 3

A

$$\text{Ras•Cdc25}^{Mm285} + \text{GDP} \rightleftharpoons \text{Ras•GDP}_L\text{•Cdc25}^{Mm285} \rightleftharpoons \textit{Ras}\text{•GDP}_T + \text{Cdc25}^{Mm285}$$

B

$$\text{Ras•Cdc25}^{Mm285} + \text{GDP} \rightleftharpoons \text{Ras•GDP}_L\text{•Cdc25}^{Mm285} \rightleftharpoons \textit{Ras}\text{•GDP}_T\text{•Cdc25}^{Mm285} \rightleftharpoons \textit{Ras}\text{•GDP}_T + \text{Cdc25}^{Mm285}$$

becomes rate-limiting. The solid lines in Figure 6A are calculated curves fitted to Scheme 2 with the rate constants shown in Table 2. Similar experiments were performed with 3′mdGDP as listed and confirm earlier findings (*23*, *33*, *34*).

When we measured the binding of nucleotides 3′mdGDP and 3′mdGTP to the binary Ras·Cdc25^{Mm285} complex, the observed association reactions were almost identical to those observed with nucleotide-free Ras (compare panels A and B of Figure 6 and Table 2). Similar to the association of nucleotide to Ras-nf, this was interpreted as a two-step reaction with the fluorescence change attributed to a second, monomolecular step. The data can indeed be fitted to such a mechanism, where the first saturable reaction has a dissociation constant of approximatively 8.5 μM for both nucleotides and represents the fast binding of nucleotide to Ras in its complex with Cdc25^{Mm285}. The interpretation of the second reaction step is less clear. Two possibilities are (i) the dissociation of Cdc25^{Mm285} from Ras·GDP (Scheme 3A) and (ii) a conformational change of Ras from a loosely binding to a tightly binding conformation, in analogy to the situation with nucleotide-free Ras alone, with a corresponding change of binding affinity of Cdc25^{Mm285} in the opposite direction. The latter (Scheme 3B) would be an extension of the kinetic scheme depicted in Scheme 3A. Here the dissociation of Cdc25^{Mm285} from its complex with Ras·GDP would be faster than the preceding conformational change and would not be measurable under the experimental conditions. We have tried to investigate the reverse reaction by measuring the association of Cdc25^{Mm285} to Ras·3′mdGDP with a stopped-flow apparatus, as done before for Ran/RCC1

Scheme 4

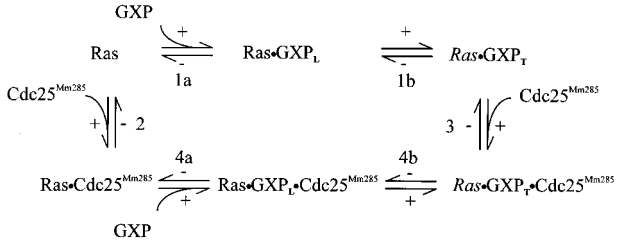

(*20*), to be able to distinguish between Schemes 3A and 3B. Unfortunately, Cdc25^{Mm285} aggregated at high concentration, as already mentioned above. We have assumed that the second step of the association of nucleotide to the Ras·-Cdc25^{Mm285} complex is a conformational change (Scheme 3B), since (i) most, if not all, association reactions involving proteins occur in two (or more) reaction steps; (ii) the constants describing the fast binding step and the following first-order reaction are strikingly similar for the association of nucleotide to Ras-nf and to Ras·Cdc25^{Mm285}; and (iii) a change in the nucleotide binding affinity is an obligatory step in the overall reaction pathway. Together with Schemes 1 and 2, this led to the complete interaction depicted in Scheme 4. Additionally we can assume that the GEF binding site on Ras undergoes a similar change from a high- to a low-affinity state to allow it to rapidly dissociate from the ternary complex.

Global Fit: Estimation of Missing Constants and Testing of the Model. The tendency of Cdc25^{Mm285} to aggregate and the inability to produce sufficient concentrations of ternary complex during the equilibrium titration did not allow an experimental determination of the parameters of some of the reaction steps. However, with the different experimental data available, one can estimate the missing constants. As reported above, the maximal Cdc25^{Mm285}-stimulated dissociation rate, and thus the rate-limiting step of the exchange reaction, is 3.9 s^{-1} for the 3′mdGDP-bound form of Ras, going from Ras·3′mdGDP via the ternary complex to the binary complex Ras·Cdc25^{Mm285} and back to the binary Ras·GDP complex which is formed in the presence of excess of

free GDP. There are two candidates for this rate-limiting step: reaction steps −4b and +3 (Scheme 4), representing the isomerization reaction of Ras in the ternary complex and the association of Cdc25^{Mm285} to Ras·3′mdGDP, respectively. Other reaction steps have been measured directly and shown to be faster than the maximal exchange rate or can be deduced to be faster. For instance, we have shown that the association of nucleotide to the binary complex Ras·Cdc25^{Mm285} has the characteristics of a two-step mechanism. Thus, on the basis of reaction Scheme 3B, it follows directly that the dissociation of Cdc25^{Mm285} from the ternary complex is faster than the onward isomerization reaction ($k_{-3} > k_{+4b}$), implying that reaction step −3 is not rate-limiting.

Although a bimolecular association reaction like step +3 is usually not rate-limiting at saturating concentrations of substrate, we cannot exclude that this association comprises a conformational change of Cdc25^{Mm285} that might become rate-limiting at high concentrations of substrate, similar to the association of nucleotide to nucleotide-free Ras or to the complex Ras·cdc25^{Mm285}. However, since we have no experimental data necessitating the extension of the reaction scheme, we have assumed reaction step −4b to be the rate-limiting step, i.e., $k_{-4b} = 3.9\ s^{-1}$ for 3′mdGDP. Subsequently, K_D4 could be calculated from the equation $K_D4 = k_{off}/k_{on} = (k_{-4b}K_D4a)/k_{+4b}$, and K_D3, from $K_D1/K_D2 = K_D4/K_D3$. This gives a K_D3 value of 0.6 (when using the K_D1 and K_D4 derived from the data of individual experiments) or 0.3 mM (when using the K_D1 and K_D4 derived from the global fit) for the Ras·3′mdGDP·Cdc25^{Mm285} complex in agreement with the results of the equilibrium titration (Figure 2): $K_D3 > 1\ \mu M$. Since $k_{-3} > k_{+4b}$, the lower limit for k_{+3} could be calculated from the K_D3 value (Table 3) to be $3.4 \times 10^4\ M^{-1}\ s^{-1}$ for the 3′mdGDP-form. Hence, according to our model, at high protein and nucleotide concentrations all reactions proceed at fast rates, with isomerization step −4b as the rate-limiting step. In the presence of a low protein concentration, however, the preceding association step (k_{+3}) will also influence the overall rate.

Figure 6 shows the calculated curves when we apply a global multiparameter fit to the data of the association reaction of 3′mdGTP to the binary complex Ras·Cdc25^{Mm285} (Table 3). In this global fit, we have extended the set of differential equations as mentioned in Material and Methods for the equilibrium titration, with additional differential equations to cover all reaction steps indicated in Scheme 4. For reactions 1a and 4a, our analysis only allowed the determination of the equilibrium constants K_D1a and K_D4a, not of the individual rate constants k_{+1a} and k_{-1a} or k_{+4a} and k_{-4a}, respectively. However, we could not obtain a good fit for our data when we assumed that k_{+1a} was lower than $10^7\ M^{-1}\ s^{-1}$ or that k_{+4a} was lower than $2 \times 10^7\ M^{-1}\ s^{-1}$. We concluded that these reactions must be faster and, with the help of the experimentally determined equilibrium constants, calculated that k_{-1a} and k_{-4a} must be larger than 72 and 90 s^{-1}, respectively.

Since we had no experimental data for the maximum exchange rate for 3′mdGTP, the value 1.1 s^{-1} for k_{-4b} (Table 3) was obtained from a global fit. The difference from the experimentally determined value of 3.9 s^{-1} for 3′mdGDP agrees well with the observed difference in activity of 1 μM of Cdc25^{Mm285} on the 3′mdGDP- and 3′mdGTP-loaded forms of Ras (Figure 1). It is clear that the fitted curves as shown in Figure 6 describe the experimental data very well, suggesting that our presumptions for the missing parameters as described above are justified. Using these calculated values, we could also identify the source of the fluorescence increase observed after 10 s. It is caused by a small quantity of GDP that apparantly remained bound to our Ras·Cdc25^{Mm285} complex during the purification procedure. The small fluorescence increase reflects the nucleotide exchange of this contamination.

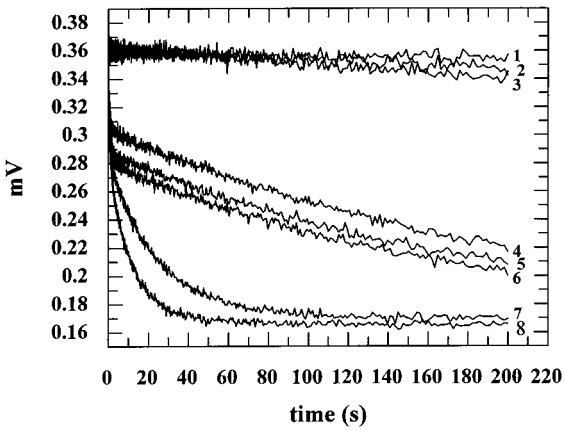

FIGURE 7: Influence of EDTA and/or Cdc25^{Mm285} on the dissociation of Ras·3′mdGDP. Ras·3′mdGDP (100 nM) was incubated in a stopped-flow apparatus with 20 μM GDP in 50 mM Tris-HCl, pH 7.6, 1 mM $MgCl_2$, and 5 mM DTE at 20 °C in the absence or presence of different concentrations and combinations of Cdc25^{Mm285} and EDTA as indicated. Trace 1, intrinsic dissociation rate; traces 2 and 3, 25 and 50 nM Cdc25^{Mm285}, respectively; traces 4, 5, and 6, 5, 10, and 15 mM EDTA, respectively; trace 7, 15 mM EDTA and 25 nM Cdc25^{Mm285}; trace 8, 15 mM EDTA and 50 nM Cdc25^{Mm285}.

It should be noted that reaction Scheme 4 comprises the minimum scheme required for the analysis of our data. As a general rule, more complicated schemes always can be used for the analysis of a given data set. For one, the binding of GEF to Ras·nucleotide may involve two or more steps, but since Cdc25^{Mm285} aggregates at high concentration, we were not able to measure this. Since the nucleotide association reaction data could be fitted well with the constants listed in Table 3, we may assume that any putative additional reaction step would be kinetically silent, at least in the time range of our experiments and using mant-nucleotides as probes.

Stimulation of Nucleotide Dissociation in the Presence of EDTA. Recently the structure of the complex between EF-Tu and EF-Ts has been solved by X-ray crystallography (*35*, *36*), where it was suggested that the guanine nucleotide exchange factor EF-Ts functions predominantly by disruption of the Mg^{2+}-binding site on EF-Tu (*35*). Since in Ras the overall rate enhancement is 10^5-fold as shown above and is only 500-fold under saturating concentrations of EDTA (*37*), we reasoned that Cdc25^{Mm285} also functions in the presence of EDTA. Figure 7 shows that in the presence of a concentration of EDTA (15 mM) sufficient to complex free and bound Mg^{2+}, Cdc25^{Mm285} is still able to significantly increase the GDP dissociation rate. This suggests that the mechanism of action of Cdc25Mm^{285} on the release of nucleotide from Ras is at least in part independent of the disruption of the metal ion binding site. The initial decrease in fluorescence that is observed in the first 100 ms of the

experiments in the presence of EDTA is due to a change in fluorescence yield following the removal of the bound Mg^{2+} ion, since it was also observed when no excess GDP was added, and thus no exchange could take place (not shown). The 30% decrease in fluorescence signal upon removal of the Mg^{2+} ion has been reported earlier (*23*).

DISCUSSION

Earlier observations with the *E. coli* EF-Tu/EF-Ts (*19*), the yeast RAS/CDC25 (*18*), the mammalian Ras/SDC25 (*17*), the Ran/RCC1 (*20*), and the Rac1/SmgGDS (*38*) systems led to the proposal that the GEF-stimulated exchange reaction in which bound GDP is replaced by GTP involves the transient formation of a ternary complex of the GTP-binding protein, nucleotide, and GEF and the formation of the stable, nucleotide-free binary complex between the GTP-binding protein and GEF. Indeed, we as well as many others have been able to isolate the binary complex (*16*, *20*, *27*, *39*−*42*; this work). Furthermore, the existence of the ternary complex was observed spectroscopically by Klebe et al. (*20*) with the Ran/RCC1 system. Similar to those studies, we show here for the Ras/Cdc25^{Mm} system that the formation of the ternary complex Ras·GXP·Cdc25^{Mm285} reduces the affinity of the nucleotide by several orders of magnitude (K_D4 versus K_D1 in Table 3).

We have shown earlier that fluorescence measurements of the dissociation rate of Ras·mGDP in the presence of Cdc25^{Mm285} give comparable values to the data obtained with radioactively labeled nucleotides (*21*). It was therefore surprising that by equilibrium titrations in solution we determine the affinity of the binary Ras·Cdc25^{Mm285} (K_D2, Table 1) as 4.6 nM, which differs by 3 orders of magnitude from the affinity found by titrating Ras·Cdc25^{Mm285} with radioactively labeled nucleotides on a nitrocellulose filter (3 pM; *16*). Such a large difference cannot be explained by differences in buffer and temperature, and it is also not due to differences in protein preparations, which were in fact very similar. The use of the fluorescent reporter has only a small influence on the kinetic and thermodynamic properties of the Ras−nucleotide interaction, as has been demonstrated by us and others (*20*, *23*, *31*, *32*, *43*, *44*), and cannot have an effect on the K_D of the Ras·Cdc25^{Mm285} complex. It was shown that the nitrocellulose filtration technique as a nonequilibrium method produces artifacts when fast reactions and/or weakly binding substrates are investigated, in particular when a stepwise reaction scheme must be considered (*45*). Proteins, but not guanine nucleotides, bind to the filters, so that the filtration process constantly changes the equilibrium of the components in the starting solution in favor of the proteins, especially when dealing with fast reactions, e.g., the formation and dissociation of the ternary complex. Since the K_D of the binary complex has been independently determined by plasmon surface resonance to be 3.3 nM, we can be confident that the affinity is indeed 3 orders of magnitude lower than reported (*16*). The lower affinity of Cdc25^{Mm285} to Ras relative to that of the nucleotide has also been documented qualitatively in other experiments. Jacquet et al. (*16*) reported that the presence of even small amounts of GDP in electrophoresis buffer inhibits formation of the binary Ras·Cdc25^{Mm285} complex in native polyacrylamide gels. Jung et al. (*46*) have shown that addition of nucleotide to the complex of glutathione−agarose-bound GST−CDC25^{GEF}(863−1275) and Ras results in an immediate release of Ras·nucleotide from the GEF, demonstrating that the affinity of Ras is higher for nucleotide than for CDC25^{GEF}.

It has been shown that guanine nucleotides bind to Ras-related proteins in a two-step reaction involving a fast initial binding and a slow isomerization reaction to a tightly bound state (*20*, *23*, *34*). It is intriguing that the association of nucleotide to the Ras·GEF complex is most consistently also interpreted as a two-step reaction, with the equilibrium constant for the first binding step (K_D4a) and the rate constant for the subsequent isomerization reaction (k_{+4b}) being very similar to those of the Ras·nucleotide association reaction (K_D1a and k_{+1b}, respectively). This led us to propose the model in which GEF binds to Ras·GXP in a fast association reaction and an isomerization takes place from a state where nucleotide is bound tightly (Ras·GXP$_T$·GEF) to a state where nucleotide is bound weakly (Ras·GXP$_L$·GEF), where the isomerization reaction indicated by k_{-4b} is the rate-limiting reaction. This means that the rate-limiting step of nucleotide dissociation from Ras alone, k_{-1b}, is accelerated by a factor of 10^5 in the ternary complex, the same factor by which the affinity of nucleotide is reduced. Although we cannot prove the model as yet, the association of nucleotide to the Ras·Cdc25^{Mm285} complex can be simulated by the parameters of the global fit based on Scheme 4 (Table 4), showing that our model is in accordance with the experimental data. Furthermore, it is intriguing to propose that the initial loosely binding conformation of nucleotide on Ras, where specific interactions with the guanine base but not the phosphate residues are established (*32*), may be structurally similar to the Cdc25^{Mm285}-induced nucleotide conformation in the ternary complex obligatory for the rapid dissociation of nucleotide.

In mammalian cells SOS- and Cdc25-type exchange factors have been cloned which all contain the conserved Cdc25 homology domain. Therefore, we believe that the mechanism of accelerating nucleotide dissociation by these GEFs is fundamentally the same for all of them. However, an important aspect of the biological system (and a difference with our in vitro system) is that Ras is membrane-bound and that the SOS-type GEF may become so after stimulation via receptor tyrosine kinases (*4*, *47*−*54*). The GRF-type proteins may be activated by other mechanisms leading to membrane localization (*55*−*58*). The activity of Cdc25^{Mm}/RasGrf in stimulating the dissociation of nucleotides from Ras was found to be higher with posttranslationally modified than with unmodified Ras (*59*, *60*), whereas Porfiri et al. could not confirm this but found that only SOS is dependent on prenylation for efficient catalysis (*61*, *62*). We find it unlikely that the prenylation of Ras or the membrane binding of GEF modifies the kinetic mechanism of nucleotide exchange discussed here, since no residues of the C-terminal end of Ras has been implicated to be involved in the Ras−GEF interaction (for references, see ref 63). However, it is certain that localization of GEF to the plasma membrane causes high local concentrations of the proteins, thus increasing the GEF activity. In support of this, it was shown that membrane targeting of the GEF by adding a CAAX-box to the C-terminal sequence potentiates the GEF activity (*64*, *65*). In addition, Quilliam et al. (*66*) have shown that membrane targetting rather than prenylation is required for

the inhibitory activity of Ras(S17N), which supposedly acts by sequestering Ras−GEF. In this context it should be noted that there are basic differences between the constants found for the Ras/Cdc25^{Mm285} and Ran/RCC1 systems. Whereas in the Ras/Cdc25^{Mm285} system high concentrations of substrate are needed to saturate the exchange reaction (Figure 2) and the affinity of Cdc25^{Mm285} for Ras·nucleotide is very low (Table 3), for the Ran/RCC1 system much lower substrate concentrations are needed to saturate the exchange reaction and the dissociation constant (K_D3) of RCC1 for Ran·nucleotide is 2 orders of magnitude smaller than the K_D3 in the Ras/Cdc25^{Mm285} system (*20*). These data strongly suggest that nature provided Ran/RCC1 with high-affinity markers, allowing the exchange reaction to take place in solution, whereas in the case of Ras/Cdc25^{Mm}, both proteins have to be membrane-bound for the exchange reaction to take place.

In our hands the Cdc25^{Mm285}-stimulated dissociation rate of Ras·GDP is only 2 times higher than that of Ras·GTP (Figure 1), which is similar to results obtained with Ran/RCC1 (*20*) and yeast proteins CDC25/RAS2 (*28*), but somewhat different from the results obtained by others in various Ras/GEF combinations (*13*, *16*, *27*). Our results support the notion that guanine nucleotide exchange factors such as Cdc25^{Mm} do not favor per se the formation of the active GTP-bound complex, but rather they catalyze the attainment of the equilibrium between the GDP-bound and the GTP-bound states, which is determined by the respective nucleotide affinities, by the concentrations of GDP and GTP in the cell, and by the concentrations of factors that bind to the GDP-bound or GTP-bound form, such as effectors, GAPs, and guanine nucleotide dissociation inhibitors. This is supported by the results on the Ran/RCC1 system, where RCC1 actually favors the formation of the GDP-bound complex by a factor of 10, consistent with the difference in affinity (*20*).

ACKNOWLEDGMENT

We thank T. Saito for providing the *E. coli* strain AD202; Christiane Theiss and Dorothee Vogt for excellent technical assistance; and Andrea Parmeggiani, Eric Jacquet, and Roger S. Goody for discussion.

REFERENCES

1. Rogge, R. D., Karlovich, C. A., and Banerjee, U. (1991) *Cell 64*, 39−48.
2. Bonfini, L., Karlovich, C. A., Dasgupta, C., and Banerjee, U. (1992) *Science 255*, 603−606.
3. Bowtell, D., Fu, P., Simon, M., and Senior, P. (1992) *Proc. Natl. Acad. Sci. U.S.A. 89*, 6511−6515.
4. Chardin, P., Camonis, J. H., Gale, N. W., Van Aelst, L., Schlessinger, J., Wigler, M. H., and Bar-Sagi, D. (1993) *Science 260*, 1338−1343.
5. Martegani, E., Vanoni, M., Zippel, R., Coccetti, P., Brambilla, R., Ferrari, C., Sturani, E., and Alberghina, L. (1992) *EMBO J. 11*, 2151−2157.
6. Shou, C., Farnsworth, C. L., Neel, B. G., and Feig, L. A. (1992) *Nature 358*, 351−354.
7. Wei, W., Mosteller, R. D., Sanyal, P., Gonzales, E., McKinney, D., Dasgupta, C., Li, P., Liu, B. X., and Broek, D. (1992) *Proc. Natl. Acad. Sci. U.S.A. 89*, 7100−7104.
8. Fam, N. P., Fan, W. T., Wang, Z. X., Zhang, L. J., Chen, H., and Moran, M. F. (1997) *Mol. Cell. Biol. 17*, 1396−1406.
9. Tanaka, S., Morishita, T., Hashimoto, Y., Hattori, S., Nakamura, S., Shibuya, M., Matuoka, K., Takenawa, T., Kurata, T., Nagashima, K., and Matsuda, M. (1994) *Proc. Natl. Acad. Sci. U.S.A. 91*, 3443−3447.
10. Gotoh, T., Hattori, S., Nakamura, S., Kiatayama, H., Noda, M., Takai, Y., Kaibuchi, K., Matsui, H., Hatase, O., Takahashi, H., Kurata, T., and Matsuda, M. (1995) *Mol. Cell. Biol. 15*, 6746−6753.
11. Van den Berghe, N., Cool, R. H., Horn, G., and Wittinghofer, A. (1997) *Oncogene 15*, 845−850.
12. Boguski, M. S., and McCormick, F. (1993) *Nature 366*, 643−654.
13. Créchet, J.-B., Poulet, P., Mistou, M.-Y., Parmeggiani, A., Camonis, J., Boy-Marcotte, E., Damak, F., and Jacquet, M. (1990) *Science 248*, 866−868.
14. Liu, B. X., Wei, W., and Broek, D. (1993) *Oncogene 8*, 3081−3084.
15. Chevallier-Multon, M. C., Schweighoffer, F., Barlat, I., Baudouy, N., Fath, I., Duchesne, M., and Tocque, B. (1993) *J. Biol. Chem. 268*, 11113−11118.
16. Jacquet, E., Baouz, S., and Parmeggiani, A. (1995) *Biochemistry 34*, 12347−12354.
17. Mistou, M. Y., Jacquet, E., Poullet, P., Rensland, H., Gideon, P., Schlichting, I., Wittinghofer, A., and Parmeggiani, A. (1992) *EMBO J. 11*, 2391−2397.
18. Powers, S., O'Neill, K., and Wigler, M. (1989) *Mol. Cell. Biol. 9*, 390−395.
19. Hwang, Y. W., and Miller, D. L. (1985) *J. Biol. Chem. 260*, 11498−11502.
20. Klebe, C., Prinz, H., Wittinghofer, A., and Goody, R. S. (1995) *Biochemistry 34*, 12543−12552.
21. Lenzen, C., Cool, R. H., and Wittinghofer, A. (1995) *Methods Enzymol. 255*, 95−109.
22. Nakano, H., Yamazaki, T., Ikeda, M., Masai, H., Miyatake, S., and Saito, T. (1994) *Nucleic Acids Res. 22*, 543−544.
23. John, J., Sohmen, R., Feuerstein, J., Linke, R., Wittinghofer, A., and Goody, R. S. (1990) *Biochemistry 29*, 6058−6065.
24. Kuhlmann, J., Macara, I., and Wittinghofer, A. (1997) *Biochemistry 36*, 12027−12035.
25. Bos, J. L. (1989) *Cancer Res. 49*, 4682−4689.
26. Leonardsen, L., DeClue, J. E., Lybæk, H., Lowy, D. R., and Willumsen, B. M. (1996) *Oncogene 13*, 2177−2187.
27. Lai, C. C., Boguski, M., Broek, D., and Powers, S. (1993) *Mol. Cell. Biol. 13*, 1345−1352.
28. Haney, S. A., and Broach, J. R. (1994) *J. Biol. Chem. 269*, 16541−16548.
29. Reinstein, J., Schlichting, I., Frech, M., Goody, R. S., and Wittinghofer, A. (1991) *J. Biol. Chem. 266*, 17700−17706.
30. John, J., Rensland, H., Schlichting, I., Vetter, I., Borasio, G. D., Goody, R. S., and Wittinghofer, A. (1993) *J. Biol. Chem. 268*, 923−929.
31. Rensland, H., Lautwein, A., Wittinghofer, A., and Goody, R. S. (1991) *Biochemistry 30*, 11181−11185.
32. Rensland, H., John, J., Linke, R., Simon, I., Schlichting, I., Wittinghofer, A., and Goody, R. S. (1995) *Biochemistry 34*, 593−599.
33. Schmidt, G., Lenzen, C., Simon, I., Deuter, R., Cool, R. H., Goody, R. S., and Wittinghofer, A. (1996) *Oncogene 12*, 87−96.
34. Simon, I., Zerial, M., and Goody, R. S. (1996) *J. Biol. Chem. 271*, 20470−20478.
35. Kawashima, T., Berthet-Colominas, C., Wulff, M., Cusack, S., and Leberman, R. (1996) *Nature 379*, 511−518.
36. Wang, Y., Jiang, Y., Meyering-Voss, M., Sprinzl, M., and Sigler, P. (1997) *Nat. Struct. Biol. 4*, 650−656.
37. John, J., Frech, M., and Wittinghofer, A. (1988) *J. Biol. Chem. 263*, 11792−11799.
38. Chuang, T. H., Xu, X., Quilliam, L. A., and Bokoch, G. M. (1994) *Biochem. J. 303*, 761−767.
39. Hwang, Y. W., Zhong, J. M., Poullet, P., and Parmeggiani, A. (1993) *J. Biol. Chem. 268*, 24692−24698.
40. Burton, J. L., Burns, M. E., Gatti, E., Augustine, G. J., and De Camilli, P. (1994) *EMBO J. 13*, 5547−5558.

41. Mosteller, R. D., Han, J., and Broek, D. (1994) *Mol. Cell. Biol. 14*, 1104−1112.
42. Poullet, P., Crechet, J. B., Bernardi, A., and Parmeggiani, A. (1995) *Eur. J. Biochem. 227*, 537−544.
43. Neal, S. E., Eccleston, J. F., Hall, A., and Webb, M. R. (1988) *J. Biol. Chem. 263*, 19718−19722.
44. Eccleston, J. F., Moore, K. J. M., Morgan, L., Skinner, R. H., and Lowe, P. N. (1993) *J. Biol. Chem. 268*, 27012−27019.
45. Berger, W., Prinz, H., Striessnig, J., Kang, H.-C., Haughland, R., and Glossmann, H. (1994) *Biochemistry 33*, 11875−11883.
46. Jung, V., Wei, W., Ballester, R., Camonis, J., Mi, S., Van Aelst, L., Wigler, M., and Broek, D. (1994) *Mol. Cell. Biol. 14*, 3707−3718.
47. Buday, L., and Downward, J. (1993) *Cell 73*, 611−620.
48. Egan, S. E., Giddings, B. W., Brooks, M. W., Buday, L., Sizeland, A. M., and Weinberg, R. A. (1993) *Nature 363*, 45−51.
49. Gale, N. W., Kaplan, S., Lowenstein, E. J., Schlessinger, J., and Bar-Sagi, D. (1993) *Nature 363*, 88−92.
50. Li, N., Batzer, A., Daly, R., Yajnik, V., Skolnick, E., Chardin, P., Bar-Sagi, D., Margolis, B., and Schlessinger, J. (1993) *Nature 363*, 85−88.
51. Olivier, J. P., Raabe, T., Henkemeyer, M., Dickson, B., Mbamalu, G., Margolis, B., Schlessinger, J., Hafen, E., and Pawson, T. (1993) *Cell 73*, 179−191.
52. Rozakis-Adcock, M., Fernley, R., Wade, J., Pawson, T., and Bowtell, D. (1993) *Nature 363*, 83−85.
53. Simon, M. A., Dodson, G. S., and Rubin, G. M. (1993) *Cell 73*, 169−177.
54. Skolnick, Y., Batzer, A., Lee, C.-H., Lowenstein, E., Mohammadi, M., Margolis, B., and Schlessinger, J. (1993) *Science 260*, 1953−1955.
55. Shou, C., Wurmser, A., Ling, K., Barbacid, M., and Feig, L. A. (1995) *Oncogene 10*, 1887−1893.
56. Farnsworth, C. L., Freshney, N. W., Rosen, L. B., Ghosh, A., Greenberg, M. E., and Feig, L. A. (1995) *Nature 376*, 524−527.
57. Mattingly, R. R., and Macara, I. G. (1996) *Nature 382*, 268−272.
58. Zippel, R., Orecchia, S., Sturani, E., and Martegani, E. (1996) *Oncogene 12*, 2697−2703.
59. Orita, S., Kaibuchi, K., Kuroda, S., Shimizu, K., Nakanishi, H., and Takai, Y. (1993) *J. Biol. Chem. 268*, 25542−25546.
60. Nakanishi, H., Kaibuchi, K., Orita, S., Ueno, N., and Takai, Y. (1994) *J. Biol. Chem. 269*, 15085−15091.
61. Porfiri, E., Evans, T., Chardin, P., and Hancock, J. F. (1994) *J. Biol. Chem. 269*, 22672−22677.
62. McGeady, P., Porfiri, E., and Gelb, M. H. (1997) *Bioorg. Med. Chem. Lett. 7*, 145−150.
63. Schweins, T., and Wittinghofer, A. (1994) *Curr. Biol. 4*, 547−550.
64. Aronheim, A., Engelberg, D., Li, N., Al-Alawi, N., Schlessinger, J., and Karin, M. (1994) *Cell 78*, 949−961.
65. Quilliam, L. A., Huff, S. Y., Rabun, K. M., Wei, W., Park, W., Broek, D., and Der, C. J. (1994a) *Proc. Natl. Acad. Sci. U.S.A. 91*, 8512−8516.
66. Quilliam, L. A., Kato, K., Rabun, K. M., Hisaka, M. M., Huff, S. Y., Campbell-Burk, S., and Der, C. J. (1994b) *Mol. Cell. Biol. 14*, 1113−1121.

BI972621J